Cellulose, proteins, starch and simple carbohydrates molecules control the hydrogen exchange capacity of bio-indicators and foodstuffs

A-L. Nivesse, N. Baglan, Gilles F Montavon, G. Granger, O. Péron

Cellulose, proteins, starch and simple carbohydrates molecules control the hydrogen exchange capacity of bio-indicators and foodstuffs.

A-L. Nivesse[1,2], N. Baglan[3], G. Montavon[1], G. Granger[1], O. Péron[1*]

[1]SUBATECH, UMR 6457, 4, rue Alfred Kastler, BP 20722, 44307 Nantes Cedex 3, France
[2]CEA, DAM, DIF, F-91297 Arpajon, France
[3]CEA, DIF, DRF, JACOB, IRCM, SREIT, LRT, F-91297 Arpajon, France
*olivier.peron@subatech.in2p3.fr

Keywords: Organically bound tritium, hydrogen exchangeability, isotopic exchange, buried tritium.

Highlights:

- The buried tritium form was detected in both a bio-indicator (water-milfoil) and a food chain sample (apple).
- The content of buried tritium was correlated with the 3D structure level of starch, cellulose, proteins and simple carbohydrates molecules associations.
- The key role of the main constituents (starch, cellulose and protein, simple carbohydrates) in influencing hydrogen exchange capacity was experimentally demonstrated.
- The impact of hydrogen exchangeability on the NE-OBT distribution on environmental matrix constituents was determined.

Abstract:

Over the past several years, it has become increasingly acknowledged that Organically Bound Tritium (OBT) is the most pertinent tritium form for understanding its behavior and distribution within the biosphere. The fate of tritium actually depends on the accessibility and exchangeability of hydrogen atoms for isotopic exchanges in natural organic matter, especially in widespread biomass biomolecules like carbohydrates or proteins. The present work is therefore aimed at providing a means for improving the knowledge of tritium speciation and distribution on environmental matrices by evaluating the impact of molecular structure of various carbohydrate molecules on OBT behavior. We are thus proposing to assess the exchange capacities of hydrogen from a gas-solid isotopic exchange methodology in wheat grains, water-milfoil and apple environmental matrices using starch, cellulose/proteins and simple carbohydrates as their respective main constituents. For wheat grains, a good agreement was obtained between experimental and theoretical values as a result of the predominantly simple molecular structure of starch. For both water-milfoil and apple, the disparities between experimental and theoretical values showed the occurrence of the buried form of tritium, correlated with the 3D molecular complexity of their main constituents. The key role played by these determinant constituents on hydrogen exchange capacity could thus be experimentally demonstrated on several environmental matrices. These distinct hydrogen exchange capacities were then proven to exert an influence on the NE-OBT distribution on environmental matrix constituents, in yielding critical information to better the understanding of tritium distribution and behavior in the environment.

1. Introduction

At the present time, tritium is one of the main radionuclides released into the environment at nuclear installations. According to current forecasts, these release rates are expected to rise due to the planned development of nuclear power plants and their fuel management methods, as well as to new tritium emitting facilities, such as the International Thermonuclear Experimental Reactor (ITER) and the Evolutionary Power Reactor (EPR). Understanding the behavior of tritium in the environment is therefore an ongoing societal issue, in recognizing this behavior to be directly related to the chemical forms of tritium, i.e. tritium speciation (ASN, 2010; IRSN, 2017). In environmental matrices, tritium is found in the form of Tissue-Free Water Tritium (TFWT) and Organically Bound Tritium (OBT) after the integration of tritiated water (HTO) during photosynthesis and metabolic processes (Diabaté and Strack, 1993; Pointurier *et al.*, 2003). Over the last decade, a focus on monitoring OBT has become a major concern in many countries for both public and regulatory assurance (Kim *et al.*, 2013; Péron *et al.*, 2016; Baglan *et al.*, 2018). OBT is typically differentiated into two pools: the exchangeable pool (E-OBT), which equilibrates with the surrounding atmosphere; and the non-exchangeable pool (NE-OBT), which is experimentally inert and remains in organic matter until its degradation (Sepall and Mason, 1961; Kim *et al.*, 2013). The latter is directly representative of the amount of tritium released into the environment during growth of the biological organism; the interest of its study lies in the ability to conduct retrospective studies of tritium release into the environment.

From an analytical standpoint, it is widely assumed that the E-OBT fraction corresponds to the tritium bound to heteroatoms, while the NE-OBT fraction corresponds to the tritium covalently bound to carbon (Mann, 1971; Kim *et al.*, 2013). Based on the molecular model, it is then possible to assign to each organic molecule a theoretical exchangeable parameter (α_{model}) from the hydrogen bound to the heteroatom pool versus total hydrogen atoms.

However, this description has been challenged since previous studies highlighted major limitations of E-OBT accessibility in environmental matrices (Sepall and Mason, 1961; Baumgartner and Donhaerl, 2004; Péron *et al.*, 2018) when comparing the theoretical (α_{model}) parameter to an experimentally determined (α_{iso}) parameter (Feng *et al.*, 1993; Péron *et al.*, 2018). Molecular conformation is thus supposedly responsible for the loss of exchange capacities from a part of the theoretically exchangeable hydrogen positions, hence the designation buried tritium (BT) (Baumgartner and Donhaerl, 2004). The IAEA (International Atomic Energy Agency) has therefore suggested in its EMRAS program (EMRAS, 2010) that the NE-OBT fraction must be defined as both covalently carbon bound tritium atoms and buried tritium atoms (Kim *et al.*, 2008; Kim *et al.*, 2013). This issue is still undergoing heated debate and requires further investigation.

The present work is therefore aimed at providing insight into tritium speciation and distribution on environmental matrices by means of evaluating the impact of molecular composition and arrangement on OBT behavior. To this end, it is being proposed herein to: (i) compare (α_{model}) and (α_{iso}) parameters and, through reliance on the knowledge of molecular structures, grasp the origin of the buried tritium form, (ii) define the exchangeable capacity of environmental matrices compared to their main constituent, and (iii) assess the NE-OBT distribution with respect to both structural and exchangeable aspects.

Starch, cellulose, proteins and simple carbohydrates are among the most widespread biomolecules of the biomass on earth and may be found under diverse molecular structures in environmental matrices (Sun and Cheng, 2002; Hopkins, 2003; Sakintuna *et al.*, 2003). Two food chain matrices, i.e. wheat grains and apples, plus a bio-indicator, water-milfoil, presenting initial anthropogenic OBT activities, have been selected while their main constituents were effectively extracted in order to represent the corresponding biomolecule types and undergo exchangeability assessments.

To access the exchangeable (α_{iso}) parameter, an original methodology based on isotopic exchange under a soft path regime has been previously developed (Péron *et al.*, 2018) and subsequently validated for exchange capacity investigations in carbohydrate molecules. Knowledge of this parameter thus yields insight into the true nature of the exchangeable hydrogen pool within a studied environmental matrix and serves to improve our understanding of OBT speciation (Nivesse *et al.*, 2020).

2. Materials and methods

2.1. Reagents and chemicals

Tritium solutions were prepared at the Subatech Laboratory using a certified and calibrated source and a low-level tritium water source "*Eau des Abatilles*" (whose HTO activity lies significantly below 0.2 $Bq.L^{-1}$ (Fourré *et al.,* 2014)).

All reagents were purchased from Fisher Scientific International and met at least ACS reagent grade (i.e. match or exceed the specifications established by the American Chemical Society). Ultrapure water (18.2 MΩ·cm resistivity at 25° and < 5 $\mu g.L^{-1}$ TOC) obtained from a Milli-Q Advantage A10® system (Merck Millipore, France) was used. The tritium contaminations from reagents were considered to be negligible since the initial tritium activities of the studied matrices were significantly higher, thus suggesting only tritium depletion could be observed.

2.2. Sample preparation

The tritium contents of environmental matrices and extracted constituents were adjusted to the same reference date of July 1, 2020 by only considering the tritium radioactive decay impact. The initial contents in organically bound tritium (OBT) within environmental matrices and extracted constituents are recorded in Table 1 *(insert Table 1 here).*

2.2.1. Wheat grains and starch

Wheat grains (Matrix A-1) from the Organically Bound Tritium (OBT) working group were previously studied as part of the work presented in Péron *et al.* (2018).

Starch (Matrix A-2) is the main component of wheat grains (Matrix A-1) and was extracted according to a procedure adapted from Verwimp *et al.* (2004), Xie *et al.* (2008) and Liu and Ng (2015). Briefly summarized, wheat flour was obtained from ground and sieved wheat grains passing through a 74-µm size sieve. Wheat flour (4 g) was suspended in 28 mL of

0.25% (v/v) NaOH, followed by 1 h of stirring prior to 10 min of centrifugation at 3900 x g. The sediment was then washed three times with deionized water by stirring for 30, 15 and 10 min respectively until final neutralization with 1 M HCl prior to 10 min of centrifugation at 3900 x g for each step. The brown fraction was removed and the white fraction was first suspended in 15 mL of deionized water then passed through a 75-µm nylon screen; approx. 20 mL of deionized water was used to wash the overs. The white extracted starch filtrate was freeze-dried for 1 week and stored under vacuum prior to further use.

2.2.2. Water-milfoil and the cellulosic wall

Water-milfoil (Matrix B-1) samples were taken from the Loire River (47°45'18.7"N, 2°28'25.3"E) 2 km downstream of the Dampierre Nuclear Power Plant (NPP) (France). The fresh samples were immediately transferred into sealed plastic bags and stored frozen. After 48 h of freezing, the samples were dehydrated by oven drying at 90°C for 2 weeks. Freeze-drying was performed for 48 h to ensure complete removal of the free water fraction, and lastly the samples were stored under vacuum.

The cellulosic wall (Matrix B-2) of water-milfoil (Matrix B-1) was recovered by extraction and elimination of the cytoplasmic fraction following a procedure adapted from Sun *et al.* (2004) and Mochochoko *et al.* (2013). Briefly summarized, freeze-dried water-milfoil were ground to pass a 1-mm size sieve, and the resultant powder (100 g) was dewaxed with toluene-ethanol (2:1 v/v) in a Soxhlet apparatus at 80°C for 6 h, followed by filtration at 63 µm and washing with ethanol (96% v/v) for 24 h. Extra washing steps with water and ethanol (96% v/v) were carried out to ensure a high degree of purification. The gradual loss of green coloration was due to chloroplast leak and representative of the effective removal of the cytoplasmic fraction. The purified powder was then allowed to dry in an oven at 90°C for 48 h, freeze-dried for 48 h and stored under vacuum.

159 *2.2.3. Apples and simple carbohydrates*

160 Apples (Matrix C-1) were sampled at a distance 2 km from the Cernavodă Nuclear Power
161 Plant (NPP) (Romania, 44°20'10.0"N 28°02'13.9"E). Fresh samples were roughly cut and
162 stored frozen for 48 h, then freeze-dried for 2 weeks, ground to pass a 1-mm size sieve and
163 stored under vacuum.

164 Simple carbohydrates (Matrix C-2) were extracted from the apples (Matrix C-1) according to
165 the procedure described in Besle and Pitiot (1976). Briefly summarized, apples were cut into
166 thin strips, and the resultant sample (20g) was extracted with 1 L ethanol (85% v/v) under
167 reflux and stirring at 80°C for 1 h. After successive filtrations at 63, 20 and 0.45 μm with
168 manufactured filters, the extracted solution was reduced using Rotavapor concentration and
169 then freeze-dried for 1 week, homogenized under dried atmosphere (RH < 10%) and stored
170 under vacuum.

171

172 **2.3. Sample characterization**

173 The samples were characterized on each studied matrix, and the composition in % by weight
174 was recorded. A broad range of common components was investigated, with certain
175 components being examined more closely by virtue of representing the specific constituents
176 of selected matrices. The common components tested were: starch, cellulose, sucrose,
177 proteins, and fat contents. For starch-type matrices, i.e. A-1 and A-2, the main essential amino
178 acids of the former were described in Péron *et al.* (2018), while the maltose and glucose
179 contents were determined in the latter by applying the AACC 76-13.01 Standard method with
180 the Total StarchKit Assay (Megazyme International Ireland Ltd. Co., Wicklow, Ireland). For
181 cellulose-type matrices, i.e. B-1 and B-2, the proportions in parietal constituents of cellulose,
182 hemicellulose and lignin were analyzed using NDF (neutral detergent fiber), ADF (acid

183 detergent fiber) and ADL (acid detergent lignin) analyses, as stated in Van Soest (1963). For
184 simple carbohydrate-type matrices, i.e. C-1 and C-2, the fructose and glucose contents were
185 also recorded.

186 For each previously analyzed component, a theoretical exchangeable parameter (α_{model}) was
187 calculated from their respective literature-based and well-known molecular formula according
188 to the analytical definition of E-OBT, i.e. hydrogen bound heteroatoms are exchangeable
189 hydrogen. On this basis, a theoretical exchangeable parameter (α_{model}) could then be
190 calculated for each matrix according to its composition in % by weight in each component
191 and its assigned unitary (α_{model}). The contribution of the mineral fraction was considered to
192 be negligible due to the low hydrogen content found in the mineral fractions of living organic
193 matrices.

194

195 **2.4. Isotopic exchange procedure**

196 The gas-solid isotopic exchange process, as described in Péron *et al.* (2018), is based on the
197 isotopic steady state between a bath of KCl-saturated solution ($\left(\frac{T}{H}\right)_{l,\ bath}$), a vapor phase
198 confined in a glove box ($\left(\frac{T}{H}\right)_{g,\ vapor}$), the water condensed at the sample surface ($\left(\frac{T}{H}\right)_{l,\ cond}$)
199 and the exchangeable organically bound tritium of the sample ($\left(\frac{T}{H}\right)_{s,\ E-OBT}$), as set forth in
200 Eq. (1):

$$\left(\frac{T}{H}\right)_{l,\ bath} = \left(\frac{T}{H}\right)_{g,\ vapor} = \left(\frac{T}{H}\right)_{l,\ cond} = \left(\frac{T}{H}\right)_{s,\ E-OBT} \quad (1)$$

201

202 As part of this description, a vapor phase has been produced from a bath containing saturated
203 KCl solutions with controlled tritium activities, for the purpose of equilibration with the

204 atmosphere contained in a glove box (RH = 85.11 ± 0.89% at T = 20°C, Plas-Labs 890-THC)
205 (see Péron *et al.* (2018) for further details).
206
207 Isotopic exchanges were separately conducted on each studied matrix following both one
208 tritium-depletion experiment with a low-level tritium bath (HTO < 0.2 $Bq.L^{-1}$) and three
209 tritium-enrichment experiments with tritium-rich baths (HTO = 120, 300 and 500 $Bq.L^{-1}$).
210 Three aliquots were extracted from each bath during the isotopic exchange step to quantify
211 the exact HTO activity. Samples were recovered from the confined glove box at days 2, 3 and
212 4 to ensure that steady state had been reached. After liquid nitrogen immersion and freeze-
213 drying, the samples were heat-treated in a tubular furnace (Eraly, France), where the organic
214 matter was transformed into carbon dioxide and combustion water (Cossonnet *et al.*, 2009;
215 CETAMA, 2013; Péron *et al.*, 2016). Bath aliquots and combustion water from the samples
216 were distilled and neutralized for pH correction, if needed, while tritium activities were
217 measured by means of liquid scintillation counting (PerkinElmer Tri-carb 3170 TR/SL) using
218 an Ultima Gold LLT cocktail. The detection limit was estimated at 3 $Bq.L^{-1}$ for a counting
219 time of 180 minutes and a blank value of 2 counts per minute. The relative uncertainty was
220 calculated based on a calibration step, according to the quench curve and systematic
221 uncertainties; this relative uncertainty typically reached 10%.
222
223 At each steady state, a mean value of the combustion water from each matrix sample
224 $\left(\frac{T}{H}\right)_{s,\ OBT}$ was obtained by averaging the sample values forming the plateau. A mean value of
225 each saline solution $\left(\frac{T}{H}\right)_{l,\ bath}$ was also derived by averaging the three bath aliquot values
226 once steady state had been reached.

3. Results

3.1. Molecular model-based theoretical exchangeable parameter (α_{model})

For each studied matrix, a theoretical exchangeable parameter (α_{model}) was calculated from the molecular model of its main components and respective experimentally determined composition in % by weight. The main essential components analyzed along with their associated (α_{model}) and distributions in % by weight in the A-1, A-2, B-1, B-2, C-1 and C-2 matrices are listed in Table 2 *(insert Table 2 here)*. The distribution in % by weight of starch (A-2) in wheat grains (A-1) was directly measured at 75.3 ± 3.7% of organic matter. Towards the cellulosic wall (B-2) in water-milfoil, this distribution was estimated at 56 ± 27% of organic matter by assuming that the entire cellulose, hemicellulose and lignin parts were recovered (40.6 ± 7.3% in water-milfoil) and moreover that the protein fraction found in the cellulosic wall was correlated with the structural proteins part without the cytoplasmic proteins part (calculated at 15.2 ± 6.8% and 22.1 ± 9.6% in water-milfoil, respectively). For simple carbohydrates (C-2), their distribution in % by weight of organic matter was calculated at 88.2 ± 5.9% in apple (C-2) due to the addition of its respective content in glucose, sucrose and fructose. The resultant calculated (α_{model}) parameters on each studied matrix are given in Table 3.

Starch and cellulose are two of the most abundant bio-macromolecules of terrestrial ecosystems. They are carbohydrate molecules of glucose monomer ($(C_6H_{10}O_5)_n$) with 3/10 hydrogen atoms bound to hydroxyl groups, hence an assigned (α_{model}) equal to 30% was adopted for these polysaccharides. Glucose and fructose are simple carbohydrate monomer molecules ($C_6H_{12}O_6$) with 5/12 hydrogen atoms bound to hydroxyl groups, explaining the assigned (α_{model}) value of 41.7%. Maltose, composed of two glucose molecules, and sucrose,

250 comprising one molecule of glucose and one of fructose, are simple carbohydrates with an
251 assigned (α_{model}) value of 36.4%.

252 Lignin is a macromolecule composed of variable polyphenolic polymer biomolecules, whose
253 structure and organization depend on the environmental physicochemical conditions of
254 formation. Lignin is mainly found with an association of proportional coumaryl, coniferyl and
255 sinapyl alcohols (Kratzl *et al.*, 1976) with (α_{model}) equal to 20, 18.2 and 15.4%, respectively.
256 Considering that the loss in hydrogen atoms bound to carbon and those bound to hydrogen
257 compensates for each unit bond, as identified in several theoretical molecular structures and
258 conformations of this biomolecule (Hopkins, 2003), the (α_{model}) value assigned to lignin was
259 estimated at 17%.

260 Hemicellulose is a cellulose-like macromolecule predominantly represented in the dual form
261 of xyloglucan ((α_{model}) = 29.2%) and arabinoxylan ((α_{model}) = 25%) (Hopkins, 2003) in
262 primary and secondary plant cell walls. In order to maintain the representativeness of these
263 two biomolecules, the (α_{model}) value assigned to hemicellulose was estimated at 27.1% for
264 our study.

265 Protein content was determined by means of total nitrogenous content quantification. Proteins
266 are made up of amino acids whose (α_{model}) values lie within a range of 23 to 58%. The
267 essential amino acids were therefore analyzed in each matrix separately. For matrix A-1, the
268 composition in % by weight is available in Péron *et al.* (2018) and the (α_{model}) for proteins
269 was calculated at 37%. For matrices B-1 and B-2, the amino acid composition was determined
270 by data available in the literature (Muztar *et al.*, 1978) and an assigned (α_{model}) for proteins
271 of 42% was estimated. For the A-2, C-1 and C-2 matrices, the protein content was considered
272 to be negligible.

Fat molecules primarily consist of carbon and hydrogen atoms with a highly negligible amount of hydrogen atoms bound to the heteroatom representation (Péron *et al.,* 2018). The (α_{model}) assigned to fat molecules is thus less than 0.1% but must still be considered when performing calculations.

3.2. Isotopic exchange-based exchangeable parameter (α_{iso})

Isotopic exchanges were conducted on each studied matrix with various T/H ratios in order to evaluate the isotopic exchangeable parameter (α_{iso}), as described in Péron *et al.* (2018). For each steady state achieved, the mean value of the combustion water from each matrix sample $\left(\frac{T}{H}\right)_{s,\ OBT}$ was plotted versus the mean value of each saline solution $\left(\frac{T}{H}\right)_{l,\ bath}$, as presented for each matrix in Figure 1 *(insert Figure 1 here)*. The slope of the linear regression obtained was therefore considered as (α_{iso}) and calculated according to Eq. (2):

$$\alpha_{iso} = \frac{\Delta\left(\frac{T}{H}\right)_{s,\ OBT}}{\Delta\left(\frac{T}{H}\right)_{l,\ bath}} \quad (2)$$

From this set-up, a wide range of isotopic exchangeable parameters (α_{iso}) was obtained on the studied environmental matrices, i.e. from 16.1 ± 0.6% to 39.6 ± 1.3%, and compared to the (α_{model}) listed in Table 3 *(insert Table 3 here)*. The standard uncertainties on (α_{iso}) parameters were calculated using the least squares method with a coverage factor k equal to 2.

3.3. Determination of the non-exchangeable organically bound tritium (NE-OBT)

Following the isotopic depletion exchange experiment, which was conducted separately on each studied matrix with a low-level tritium bath (HTO < 0.2 $Bq.L^{-1}$), the samples were devoid of exchangeable organically bound tritium (E-OBT) atoms. The remaining tritium

fraction at steady state thus relates to the non-exchangeable organically bound fraction (NE-OBT). After an adequate post-treatment, as previously described, the activities measured in the combustion waters of the three solid sample replicates were averaged to obtain a mean NE-OBT value in each analyzed matrix.

Furthermore, supplementary information provided by the gas-solid isotopic exchange process served to calculate $\left(\frac{T}{H}\right)_{s,\ NE-OBT}$ by using Eq. (3) (Péron *et al.*, 2018) obtained below:

$$\left(\frac{T}{H}\right)_{s,\ NE-OBT} = \frac{\left[\left(\frac{T}{H}\right)_{s,\ OBT} - \alpha_{iso} \times \left(\frac{T}{H}\right)_{l,bath}\right]}{(1-\alpha_{iso})} \quad (3)$$

The results produced, expressed in $Bq.L^{-1}$ of combustion water (NE-OBT ($Bq.L^{-1}$)), were converted into $Bq.kg^{-1}$ of dry matter (NE-OBT ($Bq.kg^{-1}$)) using the content in % by weight of hydrogen in each matrix ($\%H_{ech}$) as well as that in water ($\%H_{water}$) by applying Eq. (4) below:

$$\text{NE} - \text{OBT}\ (\text{Bq}.\text{kg}^{-1}) = \text{NE} - \text{OBT}\ (\text{Bq}.\text{L}^{-1}) \times \frac{\%H_{sample}}{\%H_{water}} \quad (4)$$

The measured and calculated values of NE-OBT for each studied matrix are presented in Table 4 *(insert Table 4 here)*. The uncertainties associated with the results obtained were determined by calculating the average uncertainty and the propagation of uncertainties squared using a coverage factor k equal to 2. For each matrix, these two values were similar and displayed consistent assigned values of relative uncertainties. Accordingly, only the measured values will be mentioned in the Discussion section.

4. Discussion

4.1. The impact of molecular structure on hydrogen exchangeability

Among all the matrices studied, only wheat grains (Matrix A-1) and their extracted starch (Matrix A-2) presented both isotopic exchangeable parameter results ((α_{iso}) = 31.0 ± 1.0% and (α_{iso}) = 31.1 ± 1.0%, respectively) similar to their calculated theoretical exchangeable parameters ((α_{model}) = 30.0% and (α_{model}) = 31.6%, respectively). Wheat grains are mainly composed of starch, a macromolecule comprising 25% amylose (α(1→4) bound glucose molecules) and 75% amylopectin (α(1→4) bound glucose molecules branched with α(1→6) bound glucose molecules) (Sakintuna *et al.*, 2003). These glucose polymers exhibit well-known linear and helical molecular structures with a predominantly weak crystalline area and only a few intermolecular hydrogen bonds (Tester *et al.*, 2004). It can then be assumed that the analytical point of view (i.e. based on chemical bond type) is well suited and adequate to describe OBT speciation and behavior for this specific type of environmental matrix molecular structure.

In contrast, results obtained on the other matrices studied (B-1 and C-1) showed disparities between the calculated exchangeable parameter (α_{model}) and the isotopic exchangeable parameter (α_{iso}) obtained from the vapor phase (T/H) isotopic exchange experiment. According to the state-of-the-art, the first hypothesis implies that this difference is correlated with the presence of buried tritium due to the explanation of the exchangeability phenomenon inertia derived from the local 3D structure. For this reason, such compounds are particularly prized.

Water-milfoil (Matrix B-1) yielded an isotopic exchangeable parameter ((α_{iso}) = 26.4 ± 0.5%) below the calculated theoretical exchangeable parameter ((α_{model}) = 31.5%). This

matrix is mainly composed of starch, proteins and cellulosic compounds (cellulose, hemicellulose and lignin), but only the last two are capable of presenting complex 3D molecular structures. Let's start out discussion with cellulose since it contains a long linear unbranched chain of D-glucose units linked through β(1→4)-glycosidic bonds with monomer arrangements oriented at 180°, thus promoting the formation of both intra and intermolecular hydrogen bonds and allowing for the distinction of amorphous and crystalline regions (Zugenmaier, 2001; Klemm *et al.*, 2005; Wuestenberg, 2014). This specific structural stabilization corresponds to a three-dimensional network (Nishiyama *et al.*, 2003, 2002; Jarvis, 2003), whose involvement in decreasing hydrogen exchangeability has already been discussed in Péron *et al.* (2018). In this 2018 investigative work, isotopic exchangeable parameters (α_{iso}) were observed at 13.0 ±1.0% and 21.0 ±1.0% in commercial celluloses with various crystalline ratios (with respect to (α_{model}) = 30%). The hydrogen bond phenomenon present in the crystalline regions of celluloses therefore justifies that a portion of hydrogen atoms in the theoretical exchangeable position could behave as if they were placed in non-exchangeable positions.

Such a phenomenon can also be expected with proteins possessing a three-dimensional structure. Proteins are in fact polypeptides of amino acids linked by peptide bonds occurring between a carboxyl group and an amine function (Richardson, 1981; Makhatadze and Privalov, 1995; Kim *et al.*, 2008). Each peptide bond formation thus leads to the elimination of two theoretically exchangeable hydrogen atoms from the initial molecule of two amino acid units. The three-dimensional protein structures are then defined by a pattern of hydrogen bonds between these primary chain peptide groups, with a regular geometry of mostly α-helix and β-sheet saturating all the hydrogen bond donors and acceptors in the peptide backbone (Richards, 1977; Branden and Tooze, 2012; Shulz and Schirmer, 2013). These aspects of the protein structure are then more likely to induce a drastic impact on the exchangeable

parameter of the entire protein chain, depending on the sequence length and nature of the amino acid units involved.

As such, the cellulosic wall (Matrix B-2) containing all the resultant cellulosic compounds along with a portion of the proteins (the structural proteins part) were recovered from the water-milfoil. After the compositional analyses and isotopic exchange process, a considerable gap was observed between this cellulosic wall theoretical exchangeable parameter ((α_{model}) = 29.0%) and its corresponding isotopic exchangeable parameter ((α_{iso}) = 16.1 ± 0.6%). These elements therefore enable corroborating the hypothesis of a massive impact of the cellulose and protein compounds found in environmental matrix structures on hydrogen exchangeability, i.e. the presence of crystalline parts and then three-dimensional local structures yields buried tritium.

The apples (Matrix C-1) also presented an isotopic exchangeable parameter ((α_{iso}) = 28.0 ± 1.7%) significantly below the corresponding calculated theoretical exchangeable parameter ((α_{model}) = 38.7%). This matrix is basically composed of simple carbohydrates displaying a very high theoretical exchangeability rate, with an assigned (α_{model}) value of up to 41.7% (see Table 2). However, simple carbohydrates are known to partially adopt a specific conformation in complex environmental matrices and form compact aggregates with crystal or ramified arrangements (Beevers *et al.*, 1952; Kanters *et al.*, 1977). As previously noted for water-milfoil (Matrix B-1), these crystalline regions, which are typically characterized by a hydrogen bond, may supposedly be responsible for the observed decrease of hydrogen exchangeability in apples. Ramified arrangements of sugars in environmental matrices are also assumed to contain a hydrogen bond and favor a structure hindering phenomenon that could explain the loss in hydrogen exchangeability as well.

388 To confirm this hypothesis, simple carbohydrates (Matrix C-2) were extracted from apples
389 and underwent partial destruction of their initial complex 3D structure due to solubilization
390 during the extraction process. The polar nature of simple carbohydrate molecules does indeed
391 provide them with both a property of very high solubility in water; moreover, access to a
392 substantial amount of water during the extraction process was assumed to allow for their
393 entire solubilization and dissociation from other simple carbohydrate associations (Lee *et al.*,
394 2011). It is important to note that, as opposed to other previously extracted component
395 matrices (i.e. A-2 and B-2 from A-1 and B-1) with a preserved initial structure, the simple
396 carbohydrate matrix (C-2) extraction process from Matrix C-1 was intended to trigger
397 destruction of the initial sugar structure arrangements due to solubilization. After
398 compositional analyses and the isotopic exchange process, the extracted matrix (C-2)
399 presented theoretical and experimental values closely bunched together as compared to the
400 raw (C-1) matrix, i.e. ((α_{model}) = 40.4%) versus ((α_{iso}) = 39.6 ± 1.3%). These results have
401 shown that the molecular conformation destruction of sugars leads to the opening of their
402 initial ramified structure, thus allowing the entire pool of theoretically exchangeable hydrogen
403 atoms to be accessible for isotopic exchange with the surrounding atmosphere. As such, it can
404 be assumed that the initial complex 3D structure of simple carbohydrates (Matrix C-2) in
405 apples (Matrix C-1) is responsible for the hindering phenomenon and hence for the
406 inaccessibility of a portion of the theoretically exchangeable hydrogen atoms in sugar-like
407 environmental matrices.
408
409 Whenever environmental matrices are composed of various compounds with an array of
410 complex 3D molecular conformations, such as a crystalline structure or ramified arrangement,
411 it then becomes possible to ensure that the analytical point of view (i.e. based on chemical
412 bond type) is insufficient to describe OBT speciation and behavior. In contrast, the molecules

displaying a simple molecular conformation and arrangement like starch do not appear to cause buried tritium forms in wheat grains, which allows confirming that the analytical point of view is indeed sufficient to describe the NE-OBT and E-OBT forms on starch-like environmental matrices. The inferiority or equality observed between the isotopic exchangeable parameter (α_{iso}) and the theoretical parameter (α_{model}) have therefore highlighted the relatively substantial presence or total absence of the buried tritium (BT) form depending on the molecular structure specificities and complexity of the studied environmental matrices and their main component.

4.2. Exchangeable capacity of environmental matrices and impact of NE-OBT distribution

The isotopic exchange results on extracted matrices A-2, B-2 and C-2 revealed that the structure of their constituents has exerted an influence on the global behavior of hydrogen in environmental matrices A-1, B-1 and C-1. Considering the distribution of starch (A-2) in % by weight in wheat grains (A-1) (i.e. 75.3 ± 3.7%) and the distribution of the cellulosic wall (B-2) in % by weight in water-milfoil (B-1) (i.e. 56 ± 27%), as provided in Table 4, it then appears that the isotopic exchangeable parameters (α_{iso}) of the extracted matrices directly predetermine that of the environmental matrices being studied (Table 3). The result obtained on the B-2 matrix (α_{iso}) = 16.1 ± 0.6% and the (α_{model}) of the other constituents associated with their weight distribution in B-1 would actually lead to results calculated on the exchangeability parameter $\left(\alpha_{iso_{calculated}}\right)$ for the B-1 matrix very close to the results obtained by isotopic exchange (approx. 24.2 ± 14.9% vs. an actual of 26.4 ± 0.5%). From this finding, a slight relative difference ($\alpha_{iso_{calculated}}$ deviation) of 8 ± 5% was recorded from this calculated exchangeability parameter $\left(\alpha_{iso_{calculated}}\right)$ compared to the experimental (α_{iso})

parameter on the B-1 matrix. In the case of matrices A-1 and A-2, both (α_{iso}) results were also basically equal, which exhibits the exchangeability rate control from the extracted main components. The relative difference of (α_{iso}) vs. a calculated exchangeability parameter ($\alpha_{iso_{calculated}}$) (approx. 31.1 ± 0.8%) was then determined to equal 0.4 ± 0.1%. Regarding the apple (C-1) and simple carbohydrate (C-2) matrices, the significant difference ($\alpha_{iso_{calculated}}$ deviation) of 26 ± 7% between the two parameters was directly explained by the inherent partial degradation and modification of the initial structure of simple carbohydrates during the extraction process. The extracted simple carbohydrate (C-2) molecular structure was indeed no longer representative of the initial structure inside the apple (C-1) matrix, thus preventing any establishment of a direct link between the two matrices and their respective exchangeability parameters.

From the results with starch (A-2) and cellulosic wall (B-2) as the major and determinant constituents for hydrogen exchangeability in wheat grains (A-1) and water-milfoil (B-1) respectively, an exchangeable capacity model of hydrogen in environmental matrices can then be expressed by the following formula:

$$\left(\alpha_{iso_{calculated_X}}\right) = \sum r_{x_{i-det}} \times (\alpha_{iso})_{x_{i-det}} + r_{x_i} \times (\alpha_{model})_{x_i} \quad (7)$$

where:

($\alpha_{iso_{calculated}}$) = the calculated isotopic exchangeable parameter of environmental matrix "X",

$r_{x_{i-det}}$ = the distribution in % by weight of the determinant constituent "x_{i-det}" of the matrix,

$(\alpha_{iso})_{x_{i-det}}$ = its isotopic exchangeable parameter,

r_{x_i} = the distribution in % by weight of every other "x" constituent of matrix "X",

458 $(\alpha_{iso})_{x_i}$ = the isotopic exchangeable parameter of every other "x" constituent of matrix "X".

459

460 The deviations between calculated $(\alpha_{iso_{calculated}})$ parameters and experimental (α_{iso})
461 parameters for each of the studied environmental matrices are reported in Table 3. The
462 determinant constituent x_{i-det} of an environmental matrix is then designated not only as one
463 of the main constituents but also with specific structural arrangements in the particular
464 environmental matrix.

465

466 Furthermore, the calculated distributions of the initial NE-OBT matrix on the determinant
467 extracted matrix in our present study (Table 4) would seem to display a relative trend
468 proportional to the mass distribution of the given compounds while also undergoing influence
469 from their isotopic exchangeable parameter (α_{iso}).

470 A NE-OBT recovery rate on the cellulosic wall (B-2) from water-milfoil (B-1) of 44 ± 22%
471 was thus observed with a slight downward trend for its own mass distribution in the initial
472 matrix, i.e. 56 ± 27%, thus suggesting the hypothesis that a smaller portion of the non-
473 exchangeable organically bound tritium (NE-OBT) might be located in this area rather than
474 other compounds. In displaying the lowest (α_{iso}) parameter value due to crystalline and local
475 three-dimensional structures of cellulose and proteins, the cellulosic wall (B-2) is potentially
476 subjected to a slight tritium distribution deprivation during molecular synthesis and sample
477 growth as a result of the 3D molecular complexity of these compounds. On the other hand, the
478 NE-OBT recovery rate on A-2 from A-1 of 71.0 ± 8.7% appears to conform to the mass
479 distribution of the constituent (75.3 ±3.7%), demonstrating that the exchangeability rate
480 concordance of these two matrices leads to a proportional mass distribution of the NE-OBT
481 on the raw matrix (A-1). Concerning apples (C-1) and their simple carbohydrates (C-2), the
482 structural modification of sugars during the extraction step was assumed to be responsible for

483 opening the ramified structure, hence leading to the accessibility of a pool of theoretically
484 hindered exchangeable hydrogen atoms, as translated by a higher value obtained for the
485 (α_{iso}) parameter. This phenomenon has been confirmed by the extremely low NE-OBT
486 recovery rate onto C-2 from C-1 (i.e. 47 ± 11% of recovery rate vs. a weight distribution of
487 88.2 ± 5.9%), since part of the measured NE-OBT on apple (C-1) was actually buried tritium
488 (hindered tritium form) and freed during the molecular structure modification of simple
489 carbohydrates (C-2). Consequently, this freed buried tritium recovered its exchangeability
490 capacities and behaved like E-OBT, thus ultimately leading to a lower value of NE-OBT
491 measured after isotopic exchange depletion in simple carbohydrates (C-2) compared to their
492 mass distribution in C-1.

493 It is therefore possible to affirm that the hydrogen exchangeability behavior of an
494 environmental matrix is controlled and established by one of its determinant constituents,
495 which implies a proven influence on the OBT distribution on environmental matrices.

496

5. Conclusion

The impact of molecular structure and conformation on tritium behavior has been highlighted and evaluated in both food chain and bio-indicator matrices, as well as in widespread biomolecules contained in the Earth's biomass. Theoretical (α_{model}) parameters were compared to experimentally determined (α_{iso}) parameters to understand OBT speciation of studied matrices in respect to their molecular constituent. Complex 3D molecular structures of cellulose, proteins and simple carbohydrates have been identified as responsible for the hydrogen exchangeability decrease in the water-milfoil and apple matrices. The presence of the buried tritium form was thus detected for environmental matrices containing main constituents with crystalline structures or ramified molecular arrangements, while its non-appearance was concluded in wheat grains and correlated with the simpler structure of the starch molecule. It has thus been shown that determinant constituents with specific molecular conformation have total control over the hydrogen transfer mechanisms in environmental matrices and directly establish their associated exchangeable hydrogen capacity. OBT speciation in a matrix was then found to be entirely correlated to OBT speciation in its determinant constituent. A significant influence of these structural aspects was observed on the NE-OBT distribution in environmental matrix constituents, hence providing access to critical information on remnant tritium in organic matter and tritium transfer in the environment.

Acknowledgments

This work was financed by the CEA Research Center, Subatech Laboratory, France's Loire Valley Regional Council (under the POLLUSOLS OSUNA Project) and the EDF utility company. The authors would also like to thank the members of the Environmental Laboratory

521 at the Cernavodă Nuclear Power Plant for providing the apple matrix and Gurvan Rousseau
522 from SMART Nantes laboratories for supervising water-milfoil matrix sampling.
523

References

ASN, 2010. Le livre blanc du tritium, groupes de réflexion menés de mai 2008 à avril 2010 sous l'égide de l'ASN.

Baglan, N., Cossonnet, C., Roche, E., Kim, S.B., Croudace, I., Warwick, P., 2018. Feedback of the third interlaboratory exercise organised on wheat in the framework of the OBT working group. J. Environ. Radioact. Vol. 181(1), 52–61.

Baumgartner, F., Donhaerl, W., 2004. Non-exchangeable organically bound tritium (OBT): its real nature. Anal. Bioanal. Chem. Vol. 379(2), 204–209.

Beevers, C.A., McDonald, T.R.R., Robertson, J.T., Stern, F., 1952. The crystal structure of sucrose. Acta Crystallogr. Vol. 5(5), 689–690.

Besle, J.M., Pitiot, M., 1976. Extraction et purification des glucides: application à divers aliments dérivés du soja. Ann. Biol. Anim. Biochim. Biophys. Vol. 16(5), 753–772.

Branden, C.I., Tooze, J., 2012. Introduction to protein structure. Garland Sci.

CETAMA, 2013. Analyse des radionucléides dans l'environnement - Analyse du tritium dans les matrices, méthode 384. Note Tech. CETAMA.

Cossonnet, C., Neiva Marques, A.M., Gurriaran, R., 2009. Experience acquired on environmental sample combustion for organically bound tritium measurement. Appl. Radiat. Isot. Vol. 67(5), 809–811.

Diabaté, S., Strack, S., 1993. Organically bound tritium. Health Phys. Vol. 65(6), 698–712.

EMRAS, 2010. EMRAS (Environmental Modelling of Radiological Safety) Program, Modelling the Environmental Transfer of Tritium and Carbon-14 to Biota and Man. Final Report. Tritium and Carbon-14 Working Group. IAEA Vienna Austria.

Feng, X., Krishnamurty, R.V., Epstein, S., 1993. Determination of D/H ratios of nonexchangeable hydrogen in cellulose: a method based on the cellulose-water exchange reaction. Geochem Cosmochim Acta Vol. 57, 4249–4256.

549 Fourré, E., Jean-Baptiste, P., Dapoigny, A., Ansoborlo, E., & Baglan, N. 2014. “Reference
550 waters” in French laboratories involved in tritium monitoring: how tritium-free are
551 they?. Radioprotection, Vol. 49(2), 143-145.

552 Hopkins, W.G., 2003. Physiologie végétale. Ed. Boeck Supér.

553 IRSN, 2017. Rapport Actualisation des connaissances Tritium Environnement. Ed. Inst.
554 Radioprot. Sûreté Nucl. IRSN.

555 Jarvis, M., 2003. Chemistry: cellulose stacks up. Nature Vol. 426, 611–612.

556 Kanters, J.A., Roelofsen, G., Alblas, B.P., Meinders, I., 1977. The crystal and molecular
557 structure of β-d-fructose, with emphasis on anomeric effect and hydrogen-bond
558 interactions. Acta Crystallogr. B Vol. 33(3), 665–672.

559 Kim, S.B., Baglan, N., Davis, P.A., 2013. Current understanding of organically bound tritium
560 (OBT) in the environment. J. Environ. Radioact. Vol. 126(1), 83–91.

561 Kim, S.B., Workman, W.J.G., Davis, P.A. (2008) Experimental investigation of buried
562 tritium in plant and animal tissues, Fusion Science and Technology, Vol. 54, 257-260.

563 Klemm, D., Heublein, B., Fink, H.-P., Bohn, A., 2005. Cellulose: Fascinating Biopolymer and
564 Sustainable Raw Material. Angew. Chem. Int. Ed. Vol. 44(22), 3358–3393.

565 Kratzl, K., Claus, P., Reichel, G., 1976. Reactions of lignin and lignin model compounds with
566 ozone. Tappi Vol. 59(11), 86–87.

567 Lee, J.W., Thomas, L.C., Schmidt, S.J., 2011. Investigation of the Heating Rate Dependency
568 Associated with the Loss of Crystalline Structure in Sucrose, Glucose, and Fructose
569 Using a Thermal Analysis Approach. J. Agric. Food Chem. Vol. 59(2), 684–701.

570 Liu, Y., Ng, P.K.W., 2015. Isolation and characterization of wheat bran starch and endosperm
571 starch of selected soft wheats grown in Michigan and comparison of their
572 physicochemical properties. Food Chem. Vol. 176, 137–144.

573 Makhatadze, G.I., Privalov, P.L., 1995. Energetics of protein structure. Adv. Protein Chem.
574 Vol. 47, 307–425.
575 Mann, J., 1971. Deuteration and titriation. Cellul. Cellul. Deriv. Vol. 5(4).
576 Mochochoko, T., Oluwafemi, O.S., Jumbam, D.N., Songca, S.P., 2013. Green synthesis of
577 silver nanoparticles using cellulose extracted from an aquatic weed; water hyacinth.
578 Carbohydr. Polym. Vol. 98(1), 290–294.
579 Muztar, A.J., Slinger, S.J., Burton, J.H., 1978. The chemical composition of aquatic
580 macrophytes. II. Amino acid composition of the protein and non-protein fractions.
581 Can. J. Plant Sci. Vol. 58(3), 843–849.
582 Nishiyama, Y., Langan, P., Chanzy, H., 2002. Crystal structure and hydrogen-bonding system
583 in cellulose II-beta from synchrotron X-ray and neutron fiber diffraction. J Am Chem
584 Soc Vol. 124, 9074–9082.
585 Nishiyama, Y., Sugiyama, J., Chanzy, H., Langan, P., 2003. Crystal structure and hydrogen
586 bonding system in cellulose II-alpha from synchrotron X-ray and neutron fiber
587 diffraction. Am Chem Soc Vol. 125, 14300–14306.
588 Nivesse, A.-L., Thibault de Chanvalon, A., Baglan, N., Montavon, G., Granger, G., Péron, O.,
589 2020. An overlooked pool of hydrogen stored in humic matter revealed by isotopic
590 exchange: implication for radioactive 3H contamination. Environ. Chem. Lett. Vol.
591 18(2), 475–481.
592 Péron, O., Fourré, E., Pastor, L., Gégout, C., Reeves, B., Lethi, H.H., Rousseau, G., Baglan,
593 N., Landesman, C., Siclet, F., Montavon, G., 2018. Towards speciation of organically
594 bound tritium and deuterium: Quantification of non-exchangeable forms in
595 carbohydrate molecules. Chemosphere Vol. 196(1), 120–128.
596 Péron, O., Gégout, C., Reeves, B., Rousseau, G., Montavon, G., Landesman, C., 2016.
597 Anthropogenic tritium in the Loire River estuary, France. J. Sea Res. Vol. 118, 69–76.

598 Pointurier, F., Baglan, N., Alanic, G., Chiappini, R., 2003. Determination of organically
599 bound tritium background level in biological samples from a wide area in the south-
600 west of France. J. Environ. Radioact. Vol. 68(2), 171–189.
601 Richards, F.M., 1977. Areas, volumes, packing, and protein structure. Annu. Rev. Biophys.
602 Bioeng. Vol. 6(1), 151–176.
603 Richardson, J.S., 1981. The anatomy and taxonomy of protein structure. Acad. Press Vol. 34,
604 167–339.
605 Sakintuna, B., Budak, O., Dik, T., Yöndem-makascioglu, F., Kincal, N., 2003. Hydrolysis of
606 freshly prepared wheat starch fractions and commercial wheat starch using a-amylase.
607 Chem Eng Commun Vol. 190, 883–897.
608 Sepall, O., Mason, S.G., 1961. Hydrogen exchange between cellulose and water: II.
609 Interconversion of accessible and inaccessible regions. Can. J. Chem. Vol. 39(10),
610 1944–1955.
611 Shulz, G.E., Schirmer, R.H., 2013. Principles of protein structure. Springer Sci. Bus. Media.
612 Sun, X.-F., Sun, R.-C., Su, Y., Sun, J.-X., 2004. Comparative Study of Crude and Purified
613 Cellulose from Wheat Straw. J. Agric. Food Chem. Vol. 52(4), 839–847.
614 Sun, Y., Cheng, J., 2002. Hydrolysis of lignocellulosic materials for ethanol production: a
615 review. Bioresour Technol Vol. 83, 1–11.
616 Tester, R.F., Karkalas, J., Qi, X., 2004. Starch composition, fine structure and architecture. J
617 Cereal Sci Vol. 39, 151–165.
618 Van Soest, P.V., 1963. Use of detergents in the analysis of fibrous feeds. 2. A rapid method
619 for the determination of fiber and lignin. J. Assoc. Off. Agric. Chem. Vol. 46, 829–
620 835.
621 Verwimp, T., Vandeputte, G.E., Marrant, K., Delcour, J.A., 2004. Isolation and
622 characterisation of rye starch. J. Cereal Sci. Vol. 39(1), 85–90.

623 Wuestenberg, T., 2014. Cellulose and Cellulose Derivatives. John Wiley Sons.
624 Xie, X. (Sherry), Cui, S.W., Li, W., Tsao, R., 2008. Isolation and characterization of wheat
625 bran starch. Food Res. Int. Vol. 41(9), 882–887.
626 Zugenmaier, P., 2001. Conformation and packing of various crystalline cellulose fibers. Prog
627 Polym Sci 1341–1417.

628

629

Tables

	(A-1)	(A-2)	(B-1)	(B-2)	(C-1)	(C-2)
OBT (Bq.L^{-1})	52.5 (±2.8)	32.7 (±2.5)	45.4 (±2.4)	25.6 (±1.9)	63.8 (±3.9)	14.2 (±1.9)
OBT (Bq.kg^{-1})	31.3 (±2.1)	18.4 (±2.0)	18.6 (±3.8)	11.8 (±1.6)	36.2 (±2.8)	8.9 (±1.2)

Table 1: Initial contents of organically bound tritium (OBT) in wheat grains (A-1), starch (A-2), water-milfoil (B-1), cellulosic wall (B-2), apples (C-1) and simple carbohydrates (C-2) matrices

	α_{model}	(A-1)	(A-2)	(B-1)	(B-2)	(C-1)	(C-2)
Starch	30%	75.3 (±3.7)	85.1 (±2.1)	18.1 (±1.9)	7.6 (±0.9)	0.8 (±0.1)	-
Maltose	36.4%	-	14.9 (±2.1)	-	-	-	-
Glucose	41.7%	-	0.8 (±0.2)	-	-	17.3 (±0.9)	19.0 (±2.3)
Fructose	41.7%	-	-	-	-	51.0 (±1.5)	59 (±7.1)
Sucrose	36.4%	3.6 (±0.4)	-	0.8 (±0.8)	0.1 (±0.6)	19.9 (±0.6)	22.5 (±2.7)
Cellulose	30%	4.2 (±0.9)	-	16.5 (±1.5)	21.7 (±2.3)	3.7 (±1.6)	-
Lignin	17%	-	-	13.7 (±1.8)	26.2 (±3.0)	2.6 (±0.4)	-
Hemicellulose	27.1%	-	-	10.3 (±2.5)	19 (±7)	1.6 (±4.0)	-
Protein$^{(i)}$	37%	13.9 (±1.1)	-	-	-	-	-
Protein$^{(ii)}$	42%	-	-	37.3 (±2.7)	25.1 (±2.7)	-	-
Fat	< 0.1%	3.0 (±0.9)	-	3.2 (±1.3)	0.2 (±0.9)	0.9 (±0.9)	-

Table 2: The main essential components analyzed along with their associated theoretical (α_{model}), and measured/analyzed distribution in % by weight in wheat grains (A-1), starch (A-2), water-milfoil (B-1), cellulosic wall (B-2), apples (C-1) and simple carbohydrates (C-2) matrices. $^{(i)}$ and $^{(ii)}$ are representative of wheat grains and water-milfoil protein types, respectively.

	(A-1)	(A-2)	(B-1)	(B-2)	(C-1)	(C-2)
α_{model}	30.0%	31.0%	31.5%	29.0%	38.7%	40.4%
α_{iso}	31.0 ± 1.0%	31.1 ± 1.0%	26.4 ± 0.5%	16.1 ± 0.6%	28.0 ± 1.7%	39.6 ± 1.3%
$\alpha_{iso_{calculated}}$	31.1 ± 0.8%	-	24 ± 15%	-	38 ± 10%	-
$\alpha_{iso_{calculated}}$ deviation	0.4 ± 0.1%	-	8.2 ± 5.1%	-	26 ± 7%	-

Table 3: Results of the molecular model-based theoretical exchangeable parameters (α_{model}), isotopic exchange based exchangeable parameter (α_{iso}) on wheat grains (A-1), starch (A-2), water-milfoil (B-1), cellulosic wall (B-2), apples (C-1) and simple carbohydrates (C-2) matrices, along with associated ($\alpha_{iso_{calculated}}$) parameters from extracted matrix results and the ($\alpha_{iso_{calculated}}$) deviation compared to actual (α_{iso}) parameters

	NE-OBT[(a)] ($Bq.L^{-1}$)	NE-OBT[(b)] ($Bq.L^{-1}$)	NE-OBT[(b)] ($Bq.kg^{-1}$)	NE-OBT[(b)] distribution (%)	Distribution (% by weight)
(A-1)	33.1 (±3.6)[(i)]	33.1 (±2.6)[(i)]	19.7 (±1.6)	-	
(A-2)	32.2 (±1.5)	32.7 (±2.5)	18.6 (±1.4)	71.0 (±8.7)	75.3 (±3.7)
(B-1)	33.2 (±1.2)	33.7 (±3.1)	14.4 (±1.4)	-	
(B-2)	25.3 (±1.0)	24.6 (±2.3)	11.4 (±1.1)	44 (±22)	56 (±27)
(C-1)	24.9 (±3.3)	26.4 (±2.4)	15.8 (±1.5)	-	
(C-2)	16.0 (±2.6)	13.3 (±2.8)	8.4 (±1.8)	47 (±11)	88.2 (±5.9)

Table 4: Results obtained from (a) calculated and (b) NE-OBT concentration activities on the reference date of July 1, 2020 in wheat grains (A-1), starch (A-2), water-milfoil (B-1), cellulosic wall (B-2), apples (C-1) and simple carbohydrates (C-2) matrices, plus the calculated resulting distribution of NE-OBT vs. the distribution in % by weight of the constituents. [(i)]Results adapted from Péron *et al.* (2018).

Figure

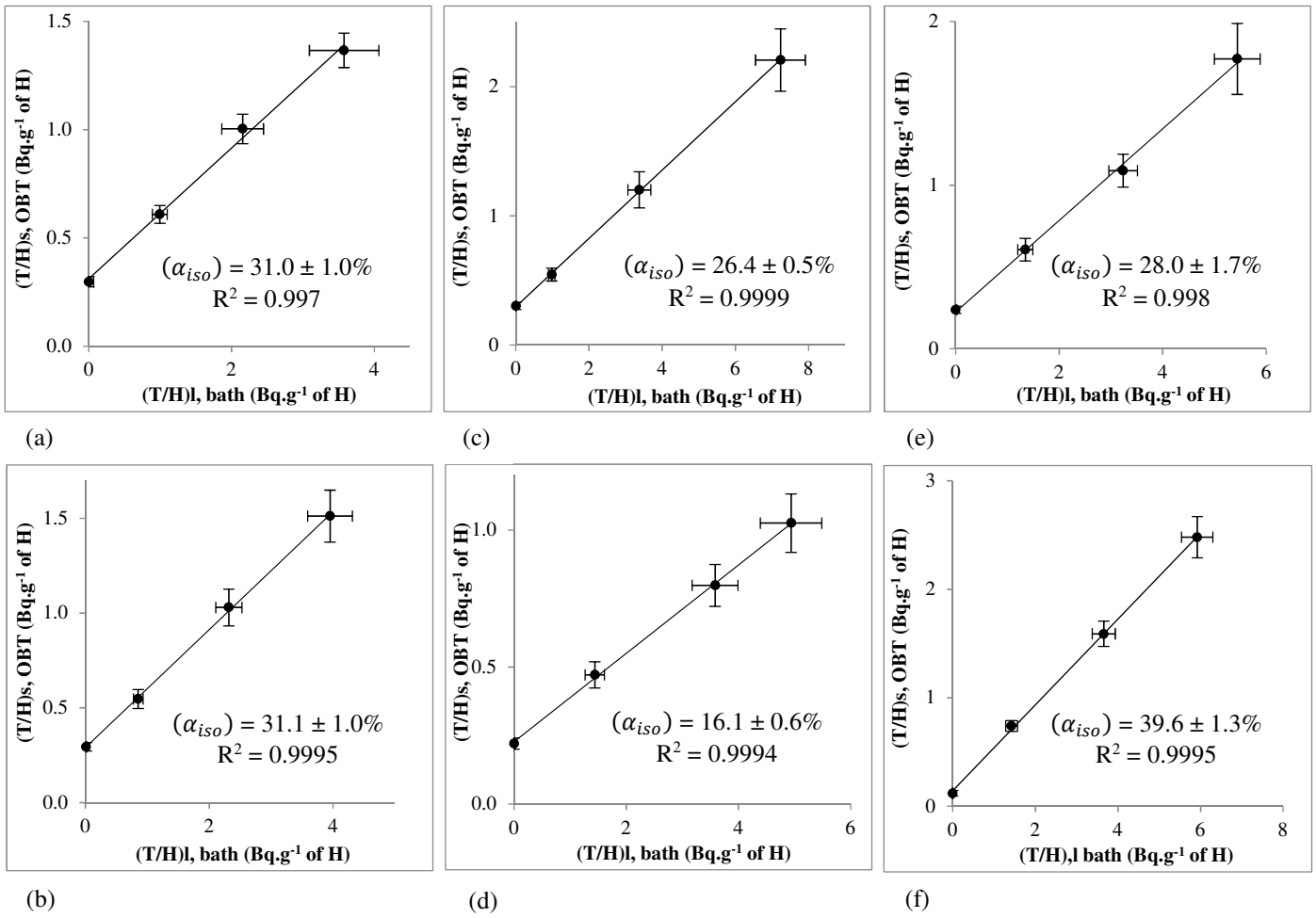

Fig. 1: (T/H) OBT at the steady state after freeze-drying vs. measured set (T/H) of saline solutions with the associated exchangeable hydrogen pool α_{iso} parameter for: (a)* wheat grains (A-1) (results from Péron *et al.* (2018)), (b) starch (A-2), (c) water-milfoil (B-1), (d) cellulosic wall (B-2), (e) apples (C-1), and (f) simple carbohydrates (C-2)